

# Doppler-shift oscillations in the H I Ly $\alpha$ coronal emission line: spectroscopic signature of propagating kink waves?

S. Mancuso<sup>1</sup> and J. C. Raymond<sup>2</sup>

<sup>1</sup> Istituto Nazionale di Astrofisica, Osservatorio Astrofisico di Torino, Strada Osservatorio 20, 10025 Pino Torinese, Italy  
e-mail: mancuso@oato.inaf.it

<sup>2</sup> Harvard-Smithsonian Center for Astrophysics, 60 Garden Street, MS 50, Cambridge, MA 02138, USA

Received 1 September 2014 / Accepted 18 November 2014

## ABSTRACT

We report the first detection of long-period, slowly decaying Doppler-shift oscillations in the H I Ly $\alpha$  (1215.67 Å) coronal emission line with the Ultraviolet Coronagraph Spectrometer (UVCS) onboard the Solar and Heliospheric Observatory (SOHO) satellite. The UV spectral data were collected at 1.43  $R_{\odot}$  above the eastern limb of the Sun during a special high-cadence sit-and-stare observation on 1997 December 14. Time-series analyses with different spectral techniques clearly show highly significant Doppler-shift oscillations in a portion with a size of 154'' of the UVCS slit that lasted for several cycles. A period of  $P = 14.3 \pm 0.4$  min was established with a confidence of better than 99.9% in the Lomb-Scargle periodogram. On average, the Doppler-shift amplitude of  $3.7 \pm 0.7$  km s<sup>-1</sup> was estimated for the most significant oscillations, roughly corresponding to a displacement of  $800 \pm 150$  km. The origin of the regular H I Ly $\alpha$  Doppler-shift oscillations is most probably due to the excitation of propagating fast magnetoacoustic kink waves along a narrow, jet-like ejection observed higher up in the white-light corona. However, different mechanisms, such as low-amplitude coherent kink oscillations of a bundle of loops along the line of sight or quasi-periodic outflows caused by oscillatory magnetic reconnection in the low corona cannot be ruled out.

**Key words.** Sun: corona – Sun: UV radiation – Sun: oscillations – Sun: coronal mass ejections (CMEs)

## 1. Introduction

Recent extreme-ultraviolet (EUV) observations in the upper solar atmosphere have revealed a plethora of small-amplitude oscillations in almost all coronal structures (see, e.g., De Moortel & Nakariakov 2012 for a review). These waves are often observed in connection with solar eruptions or flares and have the potential to provide a seismological tool for estimating local plasma parameters such as the Alfvén speed or the magnetic field strength (e.g., Nakariakov & Ofman 2001). Among the various magnetohydrodynamic (MHD) waves observed in the solar corona, kink (or transverse) oscillations with a broad range of periods (from seconds to hours) are present in most observed coronal structures. The kink mode is weakly compressive and weakly dispersive and propagates with a characteristic speed  $c_k$  given by the density-weighted average Alfvén speed inside and outside the oscillating structure (Edwin & Roberts 1982). Kink oscillations excited by nearby flares or eruptions are usually observed to rapidly decay as a result of resonant absorption (e.g., Ruderman & Roberts 2002), although decayless low-amplitude oscillations (Nisticò et al. 2013) have also been reported recently. Although most of the reported oscillations were associated with coronal loops, transverse waves have been also observed in soft X-ray solar coronal jets (e.g., Cirtain et al. 2007) with this mode, possibly excited by oscillatory magnetic reconnection (Murray et al. 2009) and interpreted in terms of fast magnetoacoustic kink modes (Vasheghani Farahani et al. 2009).

The aim of this article is to report the first detection of long-period Doppler-shift oscillations in the H I Ly $\alpha$  coronal emission line with the Ultraviolet Coronagraph Spectrometer (UVCS) onboard the Solar and Heliospheric Observatory (SOHO) satellite.

The observed properties are consistent with propagating kink waves.

## 2. Observational data

The observation analyzed in this work began at 15:08 UT and ended on the same day at 21:18 UT with exposures of 20 s each (the time interval between consecutive images was 4 to 6 s) for a total of 900 exposures. The data were collected during a dedicated, high-cadence sit-and-stare observation on 1997 December 14, with the UVCS slit centered over the east limb at a position angle of 90° and a heliocentric distance of 1.43  $R_{\odot}$ . For this observation, we used the UV spectral channel covering the 1160–1350 Å range and optimized for H I Ly $\alpha$  observations. Owing to the limited telemetry rate available to UVCS, the spectral window was confined to a 5.56 Å band centered on the Ly $\alpha$  line to achieve high spectral and spatial resolution and high image cadence. The 0.1 mm slit extended from polar angle 72.7° (−444.0'') to 107.5° (+438.0'') with data binned to 14'' (2 px) along the 882'' slit length, thus providing 64 spatial bins. Spectral binning was 1 px, yielding a spectral resolution of 0.14 Å/px with 40 bins in the dispersion direction. The latest UVCS Data Display and Analysis Software, version 5.1 (DAS51), was used to remove image distortion and to calibrate the data in wavelength and intensity.

## 3. Analysis and results

Ultraviolet lines in the corona form through collisional excitation followed by radiative de-excitation and through resonant scattering for bright enough exciting chromospheric radiation.

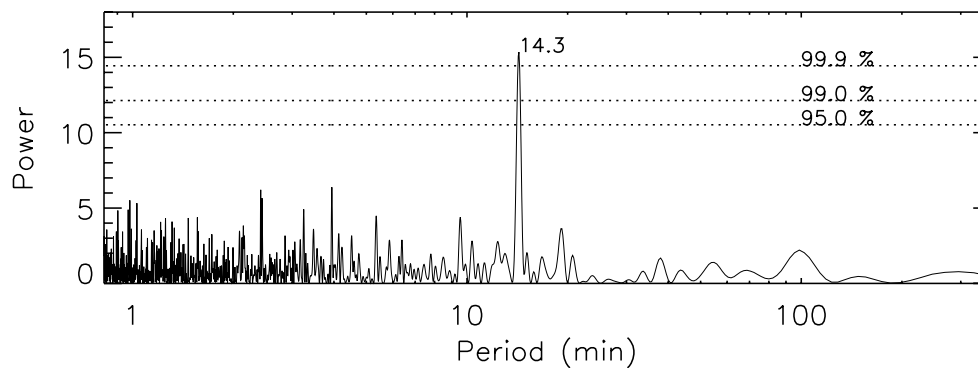


**Fig. 1.** Lomb-Scargle periodogram computed from the Doppler-shift time series integrated over the portion of the slit shown in red in Fig. 2a. Dotted lines indicate 95%, 99%, and 99.9% s.l.

The coronal H I Ly $\alpha$  emission, the strongest line observed by UVCS, forms essentially by resonant scattering (for a thorough discussion of the formation processes of this line in the corona, see Withbroe et al. 1982). The intensity of the radiatively excited component depends linearly on the l.o.s.-integrated electron density  $n_e$  as  $I_r \propto \int_{l.o.s.} n_e ds$ , but is also affected by the strength of the Doppler-shift between the incident intensity profile and the scattering line profile in the moving coronal plasma (Hyder & Lites 1970; Withbroe et al. 1982). This implies that the radiative component in stationary coronal structures is always larger than the “Doppler-dimmed” radiative component from moving plasma with the same physical characteristics.

A nonlinear least-squares fit to a Gaussian plus a constant background (e.g., Kohl et al. 1997) was performed for each 20 s exposure at each 14'' bin along the slit and for all possible binning intervals to yield the Doppler-shift, line width and Ly $\alpha$  spectral line peak intensity. To determine possible periodicities and ascertain their significance, we used a Lomb-Scargle periodogram (LSP; Scargle 1982), which allows reliably estimating the level of significance of any detected periodic signal. We performed a global analysis of the periods by computing the LSP of the detrended time series (a third-order polynomial was subtracted before the analysis) of the three parameters at all positions along the slit and by binning the data over several pixels along the spatial direction. Apart from a region 5.5° wide (11 bins  $\sim 0.16 R_\odot$ ) between 78.1° and 83.6°, we found no statistical significance  $>99\%$ . Some power just above the 95% significance level (s.l.) was found for all three parameters in a range 0.8–3.7 min all over the slit and for different spatial binning, but given the low statistical significance of the spectral peaks, they probably correspond to false detections caused by random noise. Figure 1 shows the LSP computed from the time series (Fig. 2a) obtained by measuring the Doppler-shift of the Ly $\alpha$  spectral line in the 154''-integrated portion of the slit. The solid line superposed on the time series represents the polynomial trend. The Doppler-shift shown in the plot is calculated with respect to the pre-event plasma by averaging several hours of observations before 15:08 UT. A gradually increasing, very low redshift of 2.4 km s $^{-1}$  on average (with respect to the background plasma) is inferred, suggesting a net outflow of plasma toward the observer, but very near to the plane of the sky. A highly significant oscillation is detected with a period of 14.3  $\pm$  0.4 min at a confidence  $>99.9\%$  s.l.

Wavelet analysis provides information on a time series in both time and frequency by decomposing the series using scaled and translated versions of a wavelet basis function (e.g., Torrence & Compo 1998). In Fig. 2c, we display the power of the

Morlet wavelet transform applied to the above time series. The 2D time-frequency image, which yields information on the time-varying amplitude of periodic signals within the series, shows a highly significant oscillation around 14 min lasting  $\sim 2$  h (that is, about eight oscillations) after 16 UT that is observed again (at about the same frequency) after 19 UT lasting for about another hour (about four oscillations). The wavelet power spectrum averaged over time is also shown in Fig. 2d for comparison with the LSP result together with the scale-average wavelet power in the 13 to 15 min band (Fig. 2e).

An alternative approach for time-series analysis of nonstationary, noisy data is given by the singular spectrum analysis (SSA; Vautard & Ghil 1989), a form of empirical orthogonal analysis applied in the time domain to determine autocovariance patterns in a matrix of lagged copies of a single time-series. With respect to traditional Fourier analyses, SSA allows decomposing a time series into a number of data-adaptive, nonsinusoidal components with simpler structures and is particularly successful in isolating periodic *reconstructed* components (RCs) and trends from nonstationary, noisy time series. The RCs represent the signal of interest in the time domain, the sum of all RCs returns the original time series. When we applied the SSA technique to the time series under study, we found that the only statistically significant ( $>99, 9\%$  s.l.) pair of RCs correspond to a  $\sim 14$  min oscillation (Fig. 3). All other RCs have much lower significance and are therefore compatible with background noise. On average, a Doppler-shift amplitude of  $3.7 \pm 0.7$  km s $^{-1}$  was estimated for the most significant oscillations, roughly corresponding to a displacement of  $800 \pm 150$  km. We point out, however, that the Doppler-shift amplitude is probably washed out by the contribution of foreground and background material to the Ly profile, so these must be considered as lower limits to the velocity and displacement amplitudes of the oscillations. The question arises then about the nature of the observed Doppler-shift oscillations.

#### 4. Interpretation and discussion

During the 1996–97 activity minimum, the Large Angle and Spectrometric Coronagraph (SOHO/LASCO) recorded several jet-like ejections propagating outward from the solar polar regions. Subsequent observations (Wang & Sheeley 2002) revealed that these white-light jets with an angular width of  $\sim 5^\circ$  are distributed over a much greater range of latitudes. These ejections have also been detected in O VI and H I Ly $\alpha$  spectral lines by UVCS (Dobrzycka et al. 2003). During the UVCS sit-and-stare observation, a narrow, jet-like coronal mass ejection

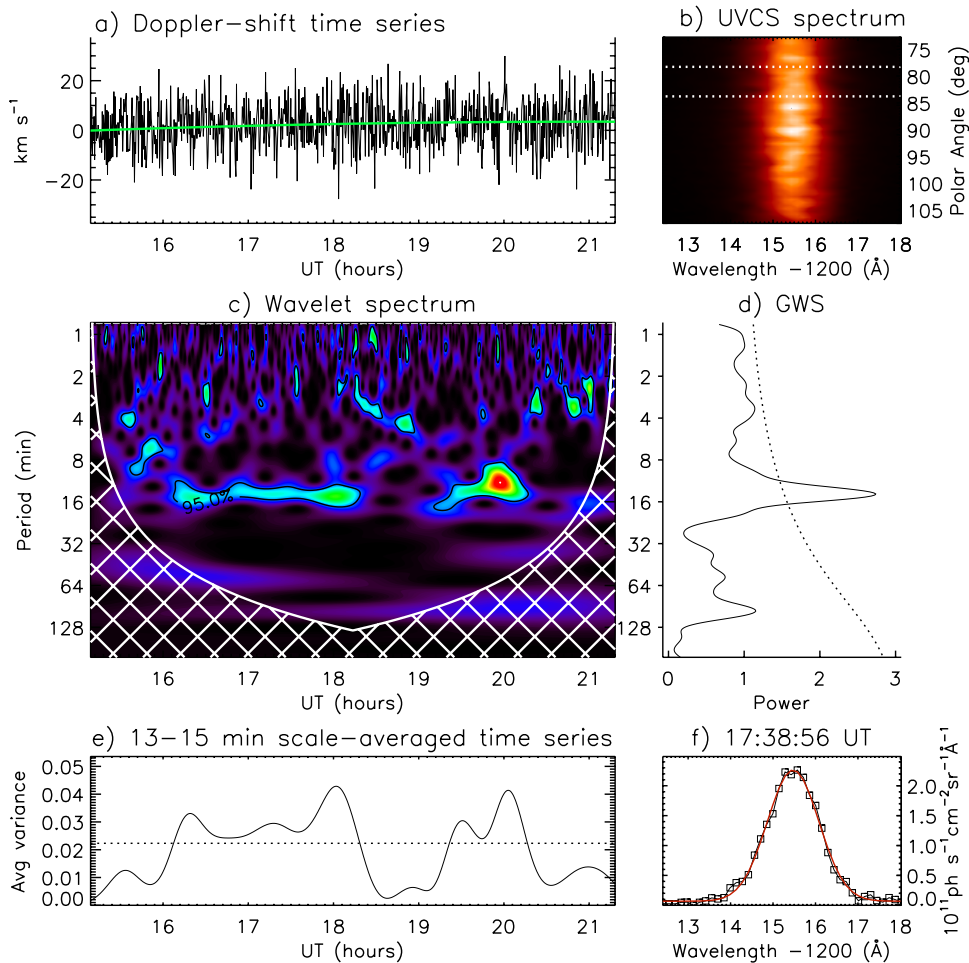


**Fig. 2.** **a)** Doppler-shift time series of the portion of the slit around  $81^\circ$ . The green line shows the polynomial fit to the trend that was subtracted before analysis. **b)** H I Ly $\alpha$  spectral line averaged over all the observation. White dotted lines delineate the edges of the portion of the slit analyzed in this work. **c)** Wavelet power spectrum. The white grid is the cone of influence (COI) or the region in which edge effects become strong. **d)** Global wavelet power spectrum. The dotted line is the 95% s.l. **e)** Scale-averaged wavelet power over the 13–15 min band. The dotted line is the 95% s.l. **f)** Example of a Gaussian fit (red curve) to the H I Ly $\alpha$  spectral line (squares).

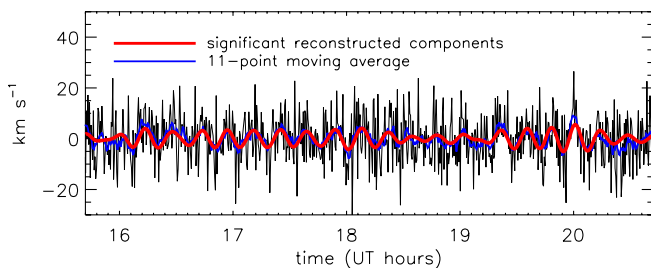


**Fig. 3.** Detrended Doppler-shift time series. Superimposed to the data, we show an 11-point moving average (blue) and an SSA reconstruction (red) of the most significant oscillation.

(CME) was observed on the east limb with LASCO. The eruption, albeit not reported in the online CME Catalog<sup>1</sup>, was centered around position angle  $80^\circ$  and visible in both LASCO C2 and C3 difference images (Fig. 4). A linear fit to the white-light height-time data yields an average speed in the plane of the sky of  $\sim 300 \text{ km s}^{-1}$  and an extrapolated onset at about 16:30 UT. The portion of the UVCS slit that showed the highest significant spectral power is spatially consistent (in position angle and width) with the observed white-light feature (see Fig. 4).

Although the oscillation seems to begin shortly before the CME onset time indicated by the linear fit to the CME height shown in Fig. 4, an initial period of acceleration preceding the constant velocity phase of the CME expansion is certainly plausible. No brightening of the Ly $\alpha$  line was observed during the CME propagation, at least within the uncertainties. This is common in UVCS observations, since coronal Ly $\alpha$  emission, which is mostly produced by resonant scattering, is strongly affected by Doppler dimming that arises from the Doppler-shift between the incident chromospheric radiation and the moving coronal plasma. The Ly $\alpha$  Doppler dimming for a plasma at  $T < 1.6 \text{ MK}$  moving at  $\sim 300 \text{ km s}^{-1}$  reduces the intensity to less than 10% of the rest velocity value. If we assume that most of the l.o.s. contribution to the observed Ly $\alpha$  intensity for a narrow CME at  $1.43 R_\odot$  is from (almost static) foreground and background plasma, then the Ly $\alpha$  enhancement along the l.o.s. could remain undetected. Unfortunately, no spectral lines other than the H I Ly $\alpha$  were available in the UVCS spectra for further analysis and diagnostics of the CME plasma.

A possible interpretation is that these Doppler-shift oscillations represent the signature of kink waves or Alfvénic waves (e.g., Tomczyk et al. 2007; Goossens et al. 2009) excited in the corona. Persistent Doppler-shift oscillations in coronal loops observed with the EUV Imaging Spectrometer onboard Hinode have been interpreted as probable spectroscopic signatures of

<sup>1</sup> <http://cdaw.gsfc.nasa.gov>

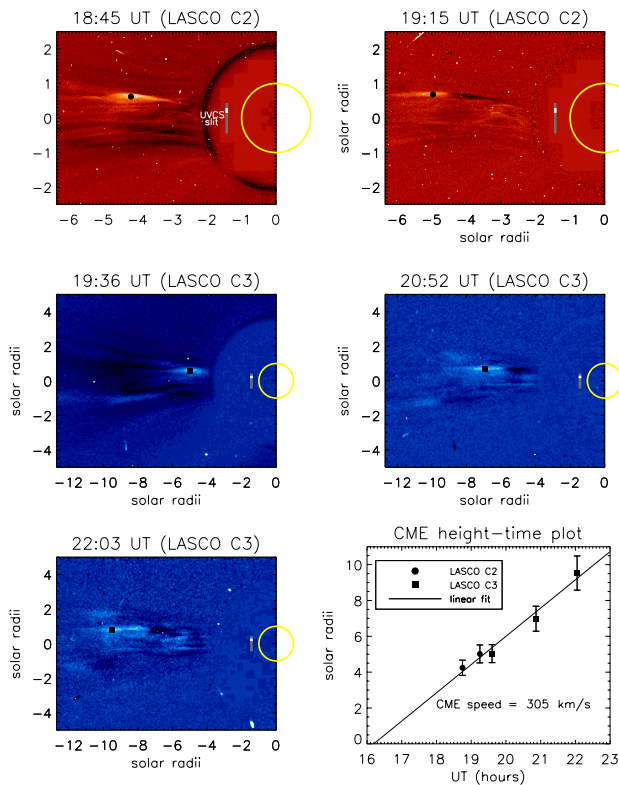


**Fig. 4.** LASCO C2 and C3 difference images of the narrow CME in 1997 on December 14. The last panel shows the CME height-time plot obtained by estimating the height of the brightest feature detected in the LASCO difference images.

kink/Alfvénic waves (Tian et al. 2012). Transverse waves observed in soft X-ray solar coronal jets (Cirtain et al. 2007) have been adequately described in terms of fast magnetoacoustic kink modes of a straight magnetic cylinder embedded in a magnetic environment (Vasheghani Farahani et al. 2009), possibly excited somewhere at the origin of the jet by Kelvin-Helmholtz instability or oscillatory magnetic reconnection (Murray et al. 2009). The interpretation of the Doppler-shift oscillations observed by UVCS as global fast magnetoacoustic kink modes fits the observational requirements quite well. They seem to be nearly incompressible, in that the upper limit to intensity fluctuations at the oscillation period is 1.7% ( $2\sigma$ ). In spectrographs such as UVCS, because of their globally coherent structure, kink modes (which are not affected by Doppler dimming) would indeed produce a periodic Doppler-shift in the spectral lines, provided there is a significant l.o.s. component of the velocity. The torsional Alfvén modes, on the other hand, do not have a collective behavior, and would show both blue- and redshifts simultaneously, thus producing a periodic nonthermal line broadening. Our analysis did not reveal periodic oscillations of the Ly $\alpha$  spectral line width at the chosen s.l. in the selected portion of the slit. We can thus exclude that the observed Doppler-shift oscillations relate to torsional Alfvén waves. Following a suggestion of the referee, it is also possible that the quasi-periodic outflows caused by oscillatory magnetic reconnection at the low corona along the narrow jet-like structure could have caused the Doppler-shift oscillations. The small amplitudes of the oscillations could then be due to projection effects, the jet being directed almost perpendicularly with respect to the l.o.s. A modest C-class flare was also observed around the projected onset time of the CME by GOES, starting at 15:23 UT, peaking at 16:11 UT, and ending at 16:39 UT (see Fig. 5), but it was probably unrelated to the

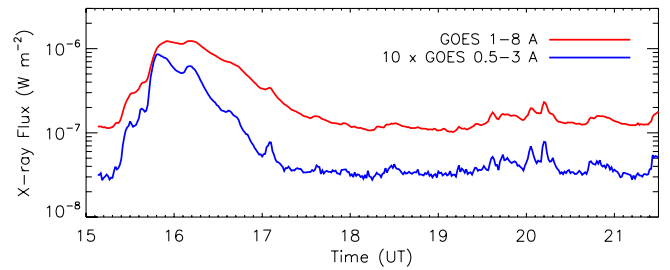


**Fig. 5.** GOES soft X-ray fluxes in 1997 on December 14: the red (blue) curve is the time profile of the GOES 1–8 (0.5–3) Å flux.

present event since it was attributed to active region AR 8122 that was located near the west limb (N29 W41), as reported in Solar Geophysical Data. The data obtained by GOES show quasi-periodic oscillations of the X-ray flux in the time interval between about 19:30 and 20:30 UT, however, where the strongest cycles of Doppler-shift oscillations were detected in the UVCS data. Modulation at times before 17 UT, when the first train of enhanced Doppler-shift amplitude in UV was detected, might have been masked by the flare activity unrelated to the present event. This suggests that the two observational signatures at different wavelengths may be somehow related and could have a common physical origin, that is, magnetic reconnection. Direct driving from a mechanism such as oscillatory magnetic reconnection (Murray et al. 2009) may thus explain both the observed 14 min period and its stability with time.

Coronal structures such as loops are also able to support different types of MHD waves that are typically induced by a nearby explosive event. Most of these oscillations, detected by EUV imagers, have been identified as impulsively generated, standing, fast magnetoacoustic kink modes with typical periods of a few to tens of minutes (e.g., White & Verwichte 2012). While short-period kink oscillations are very common, long-period oscillations  $>10$  min are less often reported (e.g., Aschwanden et al. 2002; Hori et al. 2005; Verwichte et al. 2009), although an instrumental bias against detecting long-period transverse loop oscillations can be hypothesized because of the restricted field of view of the EUV instruments. Coronal loop oscillations are generally observed to rapidly damp in the lower corona as a result of resonant absorption (Ruderman & Roberts 2002) or phase mixing (Ofman & Aschwanden 2002). On the other hand, recent observations have detected a low-amplitude fluctuating power that does not exhibit significant attenuation (Nisticò et al. 2013; Anfinogentov et al. 2013). Our observations do not rule out the possibility that we detected the signature of MHD kink modes in a bundle of coronal loop structures along the l.o.s., maybe impulsively and collectively excited by the narrow CME. Very large warm loop structures are indeed visible below the UVCS slit in the wavelet-enhanced EIT image in Fig. 6. We remark, however, that the highest s.l. of the observed periodic oscillation was observed for a slit portion much larger than the possible width of a single loop at that height. The likelihood that we observed coherent oscillations of several loops along the l.o.s., although plausible, appears somewhat speculative (see also De Moortel & Pascoe 2012 for a discussion on the effect of l.o.s. integration on an ensemble of randomly distributed loops).

## 5. Summary and conclusions

We reported the first detection of long-period, slowly decaying Doppler-shift oscillations in the H I Ly $\alpha$  coronal emission line

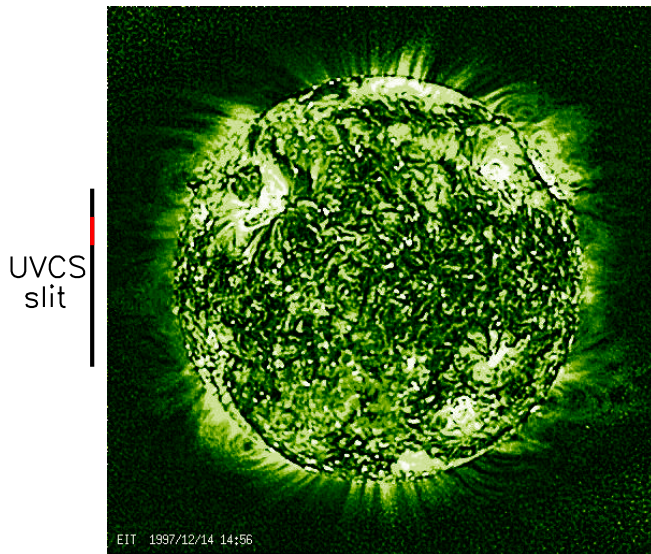


**Fig. 6.** EIT 195 Å wavelet-enhanced image of the Sun in 1997 on December 14. The UVCS slit position at  $1.43 R_{\odot}$  is shown in black. The red portion of the slit shows the area in which the 14 min Doppler-shift oscillations were detected.

observed with UVCS during a high-cadence sit-and-stare observation in 1997 on December 14, with the UVCS slit positioned at a heliocentric distance of  $1.43 R_{\odot}$ . Fourier techniques applied to the Doppler-shift time series have led to the discovery of a highly significant oscillation with a period of  $14.3 \pm 0.4$  min in a  $154''$  portion of the slit spatially consistent (in position angle and width) with the a jet-like eruption observed higher up in the white-light corona. Wavelet analysis and singular spectrum analysis of the same data independently confirmed the detection, showing a highly significant and stable oscillation of about 14 min that lasted for several cycles. Our analysis did not reveal periodic oscillations of the Ly $\alpha$  spectral line width at the chosen significance level in the selected portion of the slit, thus implying that the observed Doppler-shift oscillations were not related to torsional Alfvén waves. The origin of the regular H I Ly $\alpha$  Doppler-shift oscillations is most probably due to the excitation of propagating fast magnetoacoustic kink waves along the narrow CME observed in the white-light corona. However,

different mechanisms, such as low-amplitude coherent kink oscillations of a bundle of loops along the l.o.s. or quasi-periodic outflows caused by oscillatory magnetic reconnection in the low corona, cannot be excluded.

*Acknowledgements.* The authors would like to thank the anonymous referee for the very helpful comments and suggestions that significantly improved the paper. This work was made possible by the UVCS/SOHO instrument and Flight Operations team. The UVCS is the result of a collaborative effort between NASA and ASI, with a Swiss participation. S.M. thanks S. Rubinetti for her help in the preliminary analysis with SSA.

## References

- Anfinogentov, S. A., Nisticò, G., & Nakariakov, V. M. 2013, *A&A*, 560, A107  
 Aschwanden, M. J., De Pontieu, B., Schrijver, C. J., & Title, A. M. 2002, *Sol. Phys.*, 206, 99  
 Aschwanden, M. J., Fletcher, L., Schrijver, C. J., & Alexander, D. 1999, *ApJ*, 520, 880  
 Cirtain, J. W., Golub, L., Lundquist, L., et al. 2007, *Science*, 318, 1580  
 De Moortel, I., & Pascoe, D. J. 2012, *ApJ*, 746, 31  
 De Moortel, I., & Nakariakov, V. M. 2012, *Phil. Trans. R. Soc. A*, 370, 3193  
 Dobrzycka, D., Raymond, J. C., Biesscker, D. A., Li, J., & Ciaravella, A. 2003, *ApJ*, 588, 586  
 Edwin, P. M., & Roberts, B. 1982, *Sol. Phys.*, 76, 239  
 Goossens, M., Terradas, J., Andries, J., Arregui, I., & Ballester, J. L. 2009, *A&A*, 503, 213  
 Heyvaerts, J., & Priest, E. R. 1983, *A&A*, 117, 220  
 Hyder, C. L., & Lites, B. W. 1970, *Sol. Phys.*, 14, 147  
 Hori, K., Ichimoto, K., Sakurai, T., Sano, I., & Nishino, Y. 2005, *ApJ*, 618, 1001  
 Kohl, J. L., Esser, R., Gardner, L. D., et al. 1995, *Sol. Phys.*, 162, 313  
 Kohl, J. L., Noci, G., Antonucci, E., et al. 1997, *Sol. Phys.*, 175, 613  
 Murray, M. J., van Driel-Gesztelyi, L., & Baker, D. 2009, *A&A*, 494, 329  
 Nakariakov, V. M., & Ofman, L. 2001, *A&A*, 372, L53  
 Nakariakov, V. M., Ofman, L., Deluca, E. E., Roberts, B., & Davila, J. M. 1999, *Science*, 285, 862  
 Nisticò, G., Nakariakov, V. M., & Verwichte, E. 2013, *A&A*, 552, A57  
 Ofman, L., & Aschwanden, M. J. 2002, *ApJ*, 576, L153  
 Ruderman, M. S., & Roberts, B. 2002, *ApJ*, 577, 475  
 Scargle, J. D. 1982, *ApJ*, 263, 835  
 Tian, H., McIntosh, S. W., Wang, T., et al. 2012, *ApJ*, 759, 144  
 Tomczyk, S., McIntosh, S. W., Keil, S. L., et al. 2007, *Science*, 317, 1192  
 Torrence, C., & Compo, G. P. 1998, *Bull. Am. Meteorol. Soc.*, 79, 61  
 Vasheghani Farahani, S., Van Doorselaere, T., Verwichte, E., & Nakariakov, V. M. 2009, *A&A*, 498, L29  
 Vautard, R., & Ghil, M. 1989, *Phys. D*, 35, 395  
 Verwichte, E., Aschwanden, M. J., Van Doorselaere, T., Foullon, C., & Nakariakov, V. M. 2009, *ApJ*, 698, 397  
 Wang, Y.-M., & Sheeley, Jr., N. R. 2002, *ApJ*, 575, 542  
 White, R. S., & Verwichte, E. 2012, *A&A*, 537, A49  
 Withbroe, G. L., Kohl, J. L., Weiser, H., & Munro, R. H. 1982, *Space Sci. Rev.*, 33, 17